

Spatial Distribution of Diesel Transit Bus Emissions and Urban Populations: Implications of Coincidence and Scale on Exposure

BRIAN GOUGE,^{*,†} FRANCIS J. RIES,[†] AND HADI DOWLATABADI^{†,*,§}

Institute for Resources, Environment & Sustainability, University of British Columbia, Vancouver, British Columbia, Canada, Department of Engineering and Public Policy, Carnegie Mellon University, Pittsburgh, PA, and Resources for the Future, (RFF), Washington, D.C.

Received May 4, 2010. Revised manuscript received July 15, 2010. Accepted July 27, 2010.

Macroscale emissions modeling approaches have been widely applied in impact assessments of mobile source emissions. However, these approaches poorly characterize the spatial distribution of emissions and have been shown to underestimate emissions of some pollutants. To quantify the implications of these limitations on exposure assessments, CO, NO_x, and HC emissions from diesel transit buses were estimated at 50 m intervals along a bus rapid transit route using a microscale emissions modeling approach. The impacted population around the route was estimated using census, pedestrian count and transit ridership data. Emissions exhibited significant spatial variability. In intervals near major intersections and bus stops, emissions were 1.6–3.0 times higher than average. The coincidence of these emission hot spots and peaks in pedestrian populations resulted in a 20–40% increase in exposure compared to estimates that assumed homogeneous spatial distributions of emissions and/or populations along the route. An additional 19–30% increase in exposure resulted from the underestimate of CO and NO_x emissions by macroscale modeling approaches. The results of this study indicate that macroscale modeling approaches underestimate exposure due to poor characterization of the influence of vehicle activity on the spatial distribution of emissions and total emissions.

Introduction

Numerous studies have shown a correlation between air pollution and adverse health effects (1, 2). However, there remains significant uncertainty (2) and debate (3) surrounding the attribution of effects and the causal linkages of the emissions-to-effect impact pathway (4). Consequentially, the impact pathway has not been incorporated into the prevailing air pollution management paradigm in North America (5). Better understanding of the impact pathway will give decision and policy makers the ability to promulgate policies that more efficiently and equitably mitigate adverse health effects (5, 6).

The current management paradigm has focused on the relationship between ambient air pollution levels and health

effects at the regional scale. However, impacts are realized by individuals and inequitably distributed across populations (2). As a result there is a need to move to subregional scales that better account for personal exposure (5, 6) and heterogeneity in the spatial and temporal processes of the impact pathway (2, 7, 8).

Mobile source emissions are major contributors of air pollution (2, 9). Elevated pollutant concentrations have been found in transportation and public transportation microenvironments (10) and linked with adverse health effects (2, 11). These findings underscore the health significance of mobile source emissions and the need for increased spatial resolution to account for heterogeneity in the distribution of pollutants and impacted populations.

Macroscale emissions models such as the U.S. Environmental Protection Agency's (EPA) MOBILE model are based on emission factors that are estimates of pollutant mass emitted per unit distance traveled (9, 12). These modeling approaches have been widely applied in assessments of health and equity impacts of diesel transit bus emissions (6, 13, 14). However, these approaches do not capture the change in total emissions or the spatial variability in emissions due to the influences of driver-infrastructure interactions (9, 12, 15, 16) and vehicle mode (acceleration, deceleration, cruise, idle) (9, 12, 17).

Models such as the U.S. EPA's MOVES model are being developed to address these limitations and capture the influences of vehicle activity (9, 12, 18). These models employ microscale modeling approaches, which are based on emission rates that are estimates of pollutant mass emitted per unit time. Engine power-demand and surrogates such as vehicle specific power (VSP) have been identified as key explanatory variables of the emission rates of pollutants sensitive to mode and have been used in numerous models including MOVES (19–21).

The aim of this study was to integrate research by Zhai et al. (19) and Greco et al. (8) to investigate the implications of employing a microscale emissions modeling approach to estimate exposure to diesel transit bus emissions at a fine spatial scale (22) along one of the busiest transit corridors in Vancouver, Canada. The objectives were to quantify: (a) the spatial distribution of emissions of carbon monoxide (CO), nitrogen oxides (NO_x), and hydrocarbons (HC); (b) the relative importance of the explanatory variables of these emissions; (c) the spatial distribution of the impacted populations; and (d) the implications of the spatial relationship between emissions and impacted populations on exposure. Although studies have quantified the spatial distribution of emissions using microscale approaches (23), the authors are not aware of any previous studies that have quantified the exposure implications.

Materials and Methods

Diesel transit bus emissions were estimated in 50 m intervals along a bus rapid transit (BRT) route using a VSP-based emission rate model and vehicle activity data collected using a global positioning system (GPS) receiver. The populations impacted by the emissions were estimated from census, pedestrian, and transit ridership data in seven zones around the route. A metric was developed to quantify the change in exposure due to the spatial relationship between the emissions and impacted populations. Additional details of the methods can be found in the Supporting Information (SI).

Route and Vehicle. This study was carried out on the 99 B-Line BRT route in Vancouver, Canada (SI Figure S1). The

* Corresponding author e-mail: bgouge@interchange.ubc.ca.

† University of British Columbia.

‡ Carnegie Mellon University.

§ Resources for the Future, (RFF).

route is operated by a subsidiary of Translink, Metro Vancouver's regional transportation authority. The route was predominately serviced by 2000–1998 model year 60 ft New Flyer buses powered by Detroit Diesel Series 50 engines.

Data Collection. Vehicle activity data (time, location, and velocity) was collected using a hand-held GPS receiver that was carried on the bus. The GPS receiver was configured for a 1.0 s sampling period. A total of 61 traversals, 30 west-bound and 31 east-bound, were collected over a one week period.

Vehicle Activity Data Point. The GPS data points were transformed into vehicle activity data points for the analysis. The vehicle activity data point (Φ_k) was defined as

$$\Phi_{k=1\dots N}(t_k, d_k, g_k, v_k, a_k, VSP_k, ER_{c,k})$$

where k is the time index of the vehicle activity data point; N is the total number of data points in one traversal of the route; t_k is the time since the previous data point (s); d_k is the linear distance along the route measured from the start point (m); g_k is the grade (dimensionless); v_k is the velocity of the vehicle ($\text{m}\cdot\text{s}^{-1}$); a_k is the acceleration of the vehicle ($\text{m}\cdot\text{s}^{-2}$); VSP_k is the vehicle specific power ($\text{W}\cdot\text{kg}^{-1}$); c is the pollutant type (CO, NO_x , or HC); $ER_{c,k}$ is the emission rate ($\text{g}\cdot\text{s}^{-1}$) of pollutant c .

Sampling Interval (t_k). The sampling interval was estimated by subtracting the time-stamp of the current GPS point (k) by the time-stamp of the previous GPS point ($k-1$).

Linear Distance (d_k). The west-bound and east-bound routes were encoded using the ESRI ArcGIS linear referencing function. The bus stop at the western terminus of the routes was defined as the start point (0.0 m). Using a shortest path map-matching function, each GPS data point was mapped to a specific location on the bus routes and the linear distance from the start point, d_k , was calculated.

Road Grade (g_k). The road grade at each GPS data point was estimated using a digital elevation model (24).

Vehicle Dynamics (v_k, a_k). The velocity of each data point was estimated using unprocessed GPS data. The acceleration was estimated by differentiating velocity using the central difference numerical method.

Vehicle Specific Power (VSP_k). Vehicle specific power is defined as the instantaneous power per unit mass generated by the engine (19). It was estimated as

$$VSP_k = v_k \times (a_k + g \times \sin(g_k) + \psi) + \xi \times v_k^3 \quad (1)$$

where g is the acceleration due to gravity ($\text{m}\cdot\text{s}^{-2}$); ψ is the rolling resistance term; and ξ is the aerodynamic drag term. Typical values of the terms were estimated from the literature: $\psi = 0.092$; $\xi = 0.00011$.

Emission Rate Model ($ER_{c,k}$). Emission rates of CO, NO_x , and HC were estimated using the VSP-based emission rate model developed by Zhai et al. (19). The model defines emission rate distributions for 8 VSP modes or bins. The model was developed from a data set collected using a portable emission measurement system. The fleet analyzed consisted of 1996–1995 40 ft New Flyer diesel transit buses powered by Detroit Diesel Series 50 engines equipped with oxidation catalysts.

Total Emissions (TE). Total emissions were estimated as

$$TE_c = \sum_{k=2}^{k=N} t_k \times \text{mean}(ER_{c,k}, ER_{c,k-1}) \quad (2)$$

where TE_c are the total emissions per traversal of pollutant c (g); k is the index of the vehicle activity data point; N is the total number of data points in the traversal; t_k is the sampling interval (s); and $ER_{c,k}$ is the emission rate of pollutant c ($\text{g}\cdot\text{s}^{-1}$).

Total Interval Emissions (TIE) and Instantaneous Emission Factor. To model the spatial distribution of emissions, the bus routes were partitioned into 50 m intervals and the total interval emissions were estimated as

$$TIE_{c,i} = \sum_{K_i} t_{F_i} \times \text{mean}(ER_{c,K_i}, ER_{c,K_{i-1}}) \quad (3)$$

where $TIE_{c,i}$ are the total emissions per traversal of pollutant c in interval i (g); K_i is the set of vehicle activity data points that result in emissions in interval i ; t_{F_i} is the set of the fractions of times $t_{k=K}$ spent in interval i (s); and $ER_{c,K}$ are the set of emission rates of pollutant c ($\text{g}\cdot\text{s}^{-1}$). The times spent in the interval (t_{F_i}) were estimated using standard laws of motion.

Total interval emissions were also expressed as

$$EF_{c,i} = TIE_{c,i} \times \frac{U}{L} \quad (4)$$

where EF is the instantaneous emission factor of pollutant c in interval i ($\text{g}\cdot\text{km}^{-1}$); U is a conversion factor equal to $1000 \text{ m}\cdot\text{km}^{-1}$; and L is the interval length equal to 50 m. Emission factors were also obtained from MOBILE6.2.

Impacted Population (P). Seven zones around the route were defined (SI Figure S1). Zone 1 represented near-road pedestrian populations. Zones 2–7 were defined following the regions developed by Greco et al. (8) and represented residential populations within 0–50, 50–100, 100–200, 200–500, 500–1000, and 1000–5000 m of the route.

Zone 1. The pedestrian population within each interval was modeled using pedestrian count data collected by the City of Vancouver and transit ridership data obtained from Translink. The pedestrian counts were conducted during peak morning and afternoon periods between 2000 and 2008 and were only available at major intersections between Blanca St. and Commercial Dr. (Figure 1).

Zones 2–7. Data from the 2006 Canadian census (25) aggregated at the dissemination block level was used to estimate the impacted population in zone 2–7 (SI Figure S1). The total impacted population within each interval and zone was estimated as

$$P_{i,z} = \sum_{q=1}^{q=Q} D_q \times A_{q,z} \quad (5)$$

where $P_{i,z}$ is the impacted population associated with interval i and zone $z = 2\dots7$; q is the dissemination block index; Q is the total number of dissemination blocks; D_q is the population density of dissemination block q ($\text{people}\cdot\text{m}^{-2}$); $A_{q,z}$ is the fraction of the area of the ring defining zone z that intersects dissemination block q and is centered in interval i (m^2).

Spatial Coincidence Factor (SCF). The spatial coincidence factor (SCF) is a measure of the factor increase or decrease in exposure due to the spatial correlation or coincidence of emissions and the impacted populations. The change is measured relative to the estimate of exposure that assumes emissions and/or impacted populations are homogeneously spatially distributed (i.e., modeled at the macroscale) and accounts for spatial heterogeneity characterized by microscale modeling. It was estimated as

$$SCF_{c,z} = \sum_{i=1}^{i=M} \frac{TIE_{c,i} \times P_{i,z}}{\text{mean}(TIE_{c,i=1\dots M}) \times \text{mean}(P_{z,i=1\dots M})} \quad (6)$$

where $SCF_{c,z}$ is the spatial coincidence factor per traversal for zone z and pollutant c ; i is the interval number; M is the total number of intervals in the traversal; $TIE_{c,i}$ is the total interval emissions; and $P_{i,z}$ is the impacted population.

Uncertainty and Importance Analysis. Uncertainty analysis was used to characterize the influence of uncertainty and

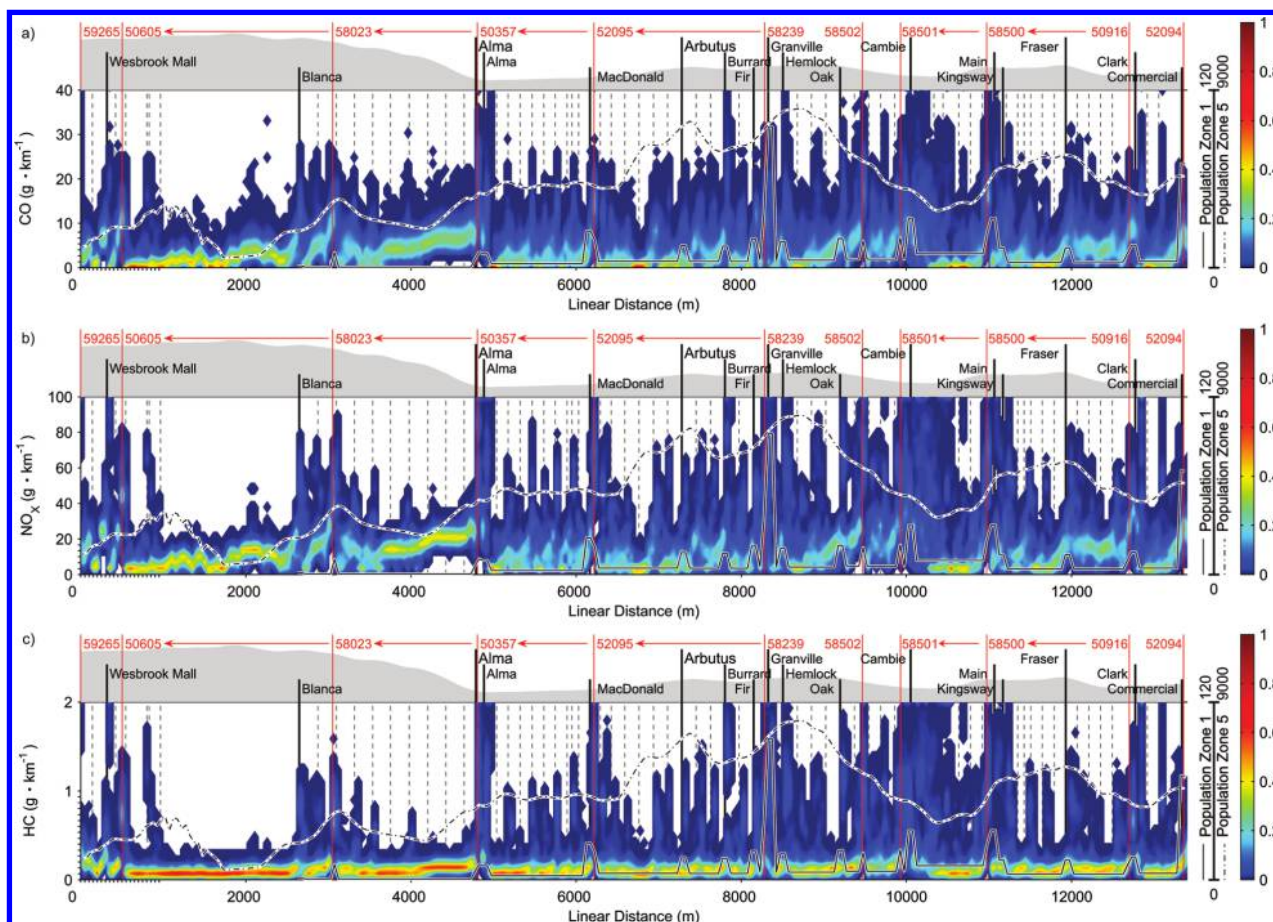


FIGURE 1. Histograms of the spatial distributions of estimated emissions of CO, NO_x, and HC for west-bound traversals of the 99 B-Line bus route. The probability of the estimated instantaneous emission factor along the route is indicated by the color bar. The direction of travel is indicated by the red arrows. Bus stops are indicated by vertical red lines. Major intersections are indicated by vertical dashed lines. The elevation is indicated by the gray profile. Populations in zone 1 (pedestrian) and zone 5 (200–500 m) are shown as indicated.

variability on the spatial distribution of emissions. SI Table S6 describes the input variable distributions and sampling methods. Each traversal was simulated 100 times. Results were based on simulated and measured traversals. Uncertainties in population estimates were not quantified.

Importance analysis was used to rank the influence of input variable uncertainty and variability on the spatial distribution of emissions. Ranks were based on partial rank correlation coefficients (PRCC). Both primary (velocity, acceleration, and grade) and secondary inputs (time and emission rate) were analyzed (SI Figure S18). Secondary inputs were functions of the primary inputs.

Results

The spatial distribution of emissions from diesel transit buses and the populations impacted by those emissions were estimated along the 99 B-Line BRT route (Figures 1 and SI S29).

Spatial Distributions of Emissions and Impacted Populations. Emissions along the route exhibited significant variability (Figures 1 and SI S29). However, there was a consistent pattern to the spatial distribution of emissions and vehicle activity over the study period (SI Figures S27 and S28). As a result of these patterns there was an increased probability of hot spots around major intersections and bus stops. Emissions and emission factors near bus stops and intersections were 1.6–3.0 times greater than the route mean (Table 1). Idle emissions made up 19–43% of the near bus stop emissions, whereas overall idle emissions made up

8–22% of total emissions (Table 1). MOBILE6.2 underestimated emissions of CO and NO_x but not HC (Table 1). The elevated emissions near Cambie St. were a result of traffic congestion and delays associated with road construction that occurred during the study period. Total emissions for west-bound traversals were higher as a result of the increased engine power-demand while traveling up the hill between Alma St. and Blanca St. (Table 1, Figure 1).

The spatial distributions of the impacted populations in the seven zones around the route are shown in Figure 1, and SI Figures S29, S20, and S21. The pedestrian population in zone 1 exhibited peaks around major intersections and bus stops. The largest peaks, at Granville St. and Commercial Dr., coincided with major transit interchanges.

Spatial Coincidence and Exposure. The coincidence of peaks in pedestrian (zone 1) populations and emission hot spots increased exposure by 20–40% (Figure 2). For populations in zones 2–7 exposure increased by 0–11%. Generally the increase in exposure was greatest for HC emissions. The underestimate of CO and NO_x emissions by MOBILE6.2 translated into an additional 19–30% increase in exposure across all zones (Table 1).

Importance. The relative importance of each of the primary input variables used to model the spatial distribution of emissions is shown in Figure 3. The high importance of acceleration indicated the distribution was sensitive to mode (Figure 3a and b), whereas the high importance of velocity indicated sensitivity to the time required to traverse an interval (Figure 3a–c). Negative PRCC values for velocity

TABLE 1. Total, Idle, Near Bus Stop and Near Intersection Emissions as well as Emissions Factors of CO, NO_x, and HC for East-Bound and West-Bound Traversals of the 99 B-Line Bus Route Estimated Using Macroscale and Microscale Modeling Approaches

| | CO | | NO _x | | HC | |
|---|-------------------------|-------------------------|-------------------------|-------------------------|-------------------------|-------------------------|
| | west | east | west | east | west | east |
| macroscale | | | | | | |
| MOBILE6.2 total emissions (g) | 49.9 | 50.7 | 188 | 191 | 3.39 | 3.44 |
| MOBILE6.2 emission factors (g·km ⁻¹) | 3.74 | 3.74 | 14.1 | 1.41 | 0.254 | 0.254 |
| error in MOBILE6.2 estimates (%) | -30 | -23 | -24 | -19 | +2.5 | +3.6 |
| microscale | | | | | | |
| total emissions (g) | 70.8 (0.059) | 65.4 (0.064) | 249 (0.064) | 235 (0.073) | 3.3 (0.089) | 3.32 (0.11) |
| mean emission factors (g·km ⁻¹) ^b | 5.31 (0.059) | 4.83 (0.064) | 18.7 (0.064) | 17.4 (0.074) | 0.248 (0.089) | 0.245 (0.11) |
| near bus stop emission factors (g·km ⁻¹) ^c | 11.4 (0.082) | 11.9 (0.10) | 42.2 (0.086) | 45.2 (0.10) | 0.651 (0.12) | 0.743 (0.13) |
| near intersection emission factors ^c | 8.61 (0.13) | 8.14 (0.13) | 30.9 (0.13) | 29.8 (0.14) | 0.434 (0.17) | 0.441 (0.17) |
| percent idle emissions (%) | 8.44 (1.8) ^a | 9.65 (2.2) ^a | 11.0 (2.1) ^a | 12.4 (2.6) ^a | 19.9 (3.1) ^a | 21.7 (3.8) ^a |
| percent idle emissions near bus stops (%) ^c | 19.2 (4.7) ^a | 24.4 (5.7) ^a | 23.9 (5.1) ^a | 29.4 (6.0) ^a | 37.7 (6.2) ^a | 43.2 (6.7) ^a |

^a Standard deviation shown in brackets. ^b Mean instantaneous emission factor (EF) estimate over the route. ^c Near is defined as within 50 m.

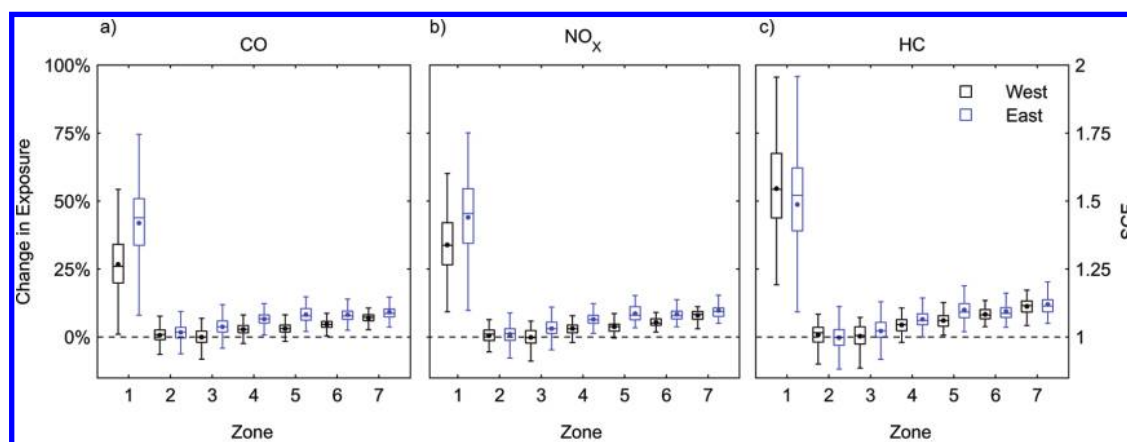


FIGURE 2. Boxplots of the spatial coincidence factor (SCF) showing the change in exposure due to the spatial coincidence of the impacted populations in seven zones around the route and estimated emissions of CO, NO_x, and HC for west-bound and east-bound traversals of the 99 B-Line bus route. Median values are indicated by bars and mean values by dots. Changes in exposure due to MOBILE6.2 underestimates are not shown.

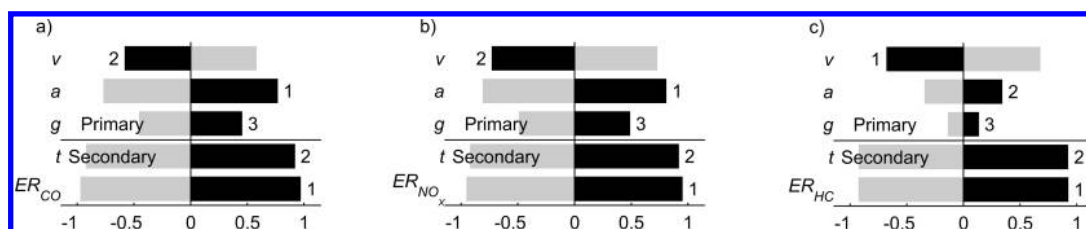


FIGURE 3. Importance analysis of the input variables used to estimate the spatial distribution of emissions of CO (a), NO_x (b), and HC (c) along the 99 B-Line bus route. Black bars indicate the partial rank correlation coefficients (PRCC) values for primary input variables: velocity (*v*), acceleration (*a*), and grade (*g*) and secondary input variables: interval traversal time (*t*) and emission rate (*ER*). Gray bars indicate negative PRCC values. Numerical rankings of importance were based on the absolute values of the PRCC. Lower ranks indicated greater importance.

indicated that total interval emissions decreased with increasing velocity. Overall, velocity, acceleration, and grade were important explanatory variables of CO and NO_x distributions, whereas velocity was the dominant explanatory variable of HC distributions. Analysis of the secondary input variables showed that regardless of the predictive power of the emissions rate model (i.e., importance was based on combined variability and uncertainty), the time required to traverse an interval and the emission rate were equally important in determining the spatial distribution of emis-

sions. This was also reflected in the fact that acceleration and velocity had similar levels of importance for emissions of CO and NO_x, which were well-predicted by the emissions rate model (Figure 3a,b).

Discussion

The emissions-to-effect impact pathway describes the causal processes by which emissions disperse and transform to form concentrations that individuals come into contact with,

resulting in exposure, intake, dose, and health effects (4). Regional scale assessments that do not account for spatial heterogeneity in these processes have been shown in this study and others to underestimate exposure (2, 7, 8) and poorly characterize the distribution of impacts over the population (2, 6).

Emissions Modeling. *Explanatory Variables.* Macroscale emissions modeling approaches such as MOBILE that employ mass per unit distance emission factors are limited in their ability to characterize heterogeneity in the spatial distribution of emissions. Furthermore, these approaches have been found in this and previous studies (9, 12) to underestimate emissions of pollutants that are sensitive to mode, such as CO and NO_x (Table 1). Microscale modeling approaches that employ mass per unit time emission rates can be combined with activity data to address these limitations. Even if the emissions rate model has little predictive power (e.g., HC emissions), significant insights into the spatial distribution of emissions may be gained from the activity data alone.

Numerous factors have been shown to influence emissions from heavy-duty diesel vehicles (17, 26). For a given vehicle configuration, engine power-demand and surrogates such as VSP have been found to be strong explanatory variables of emission rates for CO, NO_x, and particulate matter (PM) but not HC (19–21). As a result, estimates of HC emissions were associated with greater uncertainty than CO and NO_x (Table 1).

Due to the significant health effects attributed to PM exposure (2, 3), a drawback of current microscale modeling approaches is the lack of PM emissions models and data (20, 21). However, there is some evidence that CO and PM mass emission rates are correlated (27). If this is the case, the spatial distributions of the two pollutants would be similar, as well as the exposure implications and SCF estimates.

Importance of Explanatory Variables. The consistent spatial patterns of emissions modeled over the study period were a result of terrain and patterns in driver-infrastructure interactions that determined the time required for a bus to traverse an interval, the engine power-demand and the emission rate (Figure 3). However, the results of the importance analysis are contextual and quantify importance over the entire route. Analyses performed on specific intervals along the route or on different routes would potentially yield different results. For example, grade would not be an important input variable on intervals or routes without hills.

The importance analysis results applied only for buses in motion because the time required to traverse an interval could not be estimated from the primary input variables when the velocity was zero. To address this limitation, emissions within 50 m of bus stops and major intersections were analyzed in greater detail. Idle emissions made up a significant fraction of these emissions (Table 1). Thus, hot spots observed at these locations were not only the result of increased emission rates associated with acceleration and high engine power-demand (28), but also the time buses spent in these areas. In fact, hot spots were more distinct for pollutants that are not sensitive to mode, such as HC. Pollutants sensitive to mode, such as CO and NO_x, were “smeared” in the direction of travel, resulting in less distinct hot spots (Figure 1).

Uncertainty and variability of input variables were not distinguished in this analysis. Because the GPS data were of high quality and uncertainties of the primary input variables were small relative to their variability this was not expected to have a significant impact on the results (SI Figures S9 and S10).

Receptor and Population Modeling. There are significant challenges associated with modeling impacted populations, particularly at fine spatial scales. The limitations of census data have been previously discussed by Greco et al. (8). By

incorporating pedestrian counts at intersections and transit ridership data some of these limitations were addressed, but these data provided only a first-order characterization of the pedestrian population. The underlying assumption of the pedestrian model was that bus stops and major intersections introduce delays in pedestrian movements which cause pedestrians to concentrate in these areas (22). However, there are other features in the urban environment that may have similar influences.

Exposure and Spatial Heterogeneity. Intake fraction (iF) (a metric which relates the amount of pollutant inhaled to the amount emitted) has been widely employed to characterize exposure to emissions from mobile sources including diesel transit buses (4, 6, 8, 13, 14, 29). The SCF was derived from the spatially variant parameters of the iF to quantify the change in exposure due to the spatial coincidence of emissions and impacted populations, (Supporting Information). In this study only emissions and impacted populations were considered spatially variant. Meteorology and other parameters affecting dispersion were assumed to be spatially invariant (8). Although there are limitations associated with this approach, it allowed the SCF to be estimated for each zone without modeling dispersion.

The zones (modeled as areas of constant concentration) were defined so as to capture the pollutant concentration gradient across them (8). The change in total exposure (not quantified in this study) estimated across all zones would depend on this gradient. If concentrations proximate to the route were significantly elevated, as commonly reported (2, 8, 30), then the change in total exposure could be significant despite smaller populations proximate to the route.

The increase in exposure due to spatial coincidence (SCF > 1.0) experienced by pedestrian populations in zone 1 occurred because these populations were assumed to be under similar infrastructure influences (e.g., delays at intersections) as the buses and thus concentrated at locations of emission hotspots.

It was more difficult to attribute changes in exposure (SCF) to specific terrain or infrastructure features in zones 2–7. At greater distances from the route the spatial variability in emissions observed on the route was reduced through the process of dispersion and the pollutant concentrations were more spatially homogeneous. As a result both the variability in the change in exposure and the mean change in exposure were greater in zone 1 than zones 2–7 (Figure 2).

The change in exposure in zones 2–7 was due largely to the overall trend in emissions and impacted populations, which were generally lower over the western (left) section of the route than the eastern (right) section. As a result of this west-east spatial coincidence, there was approximately a 10% increase in exposure in zone 7. The west-east trend in population decreased over zones 6–2 (SI Figures S20 and S21) and as a result the change in exposure over zones 6–2 tended to 0% (Figure 2). The decrease in the change in exposure over zones 6–2 may also be due to lower residential populations around major intersections and corresponding emission hot spots. Presumably this was due to the increased commercial space around major intersections, which would have populations that are not reflected in residential census data.

The greatest increase in exposure due to spatial coincidence occurred for HC emissions in zone 1 (Figure 2). The increase was smaller for emissions sensitive to mode, such as CO and NO_x, because the smearing of these emissions had the counterintuitive effect of reducing the magnitude of hotspots.

In addition to the increase in exposure due to spatial coincidence, exposure to CO and NO_x emissions were further

increased over all zones because macroscale modeling approaches underestimated total emissions of these pollutants.

Implications and Recommendations. Compared to microscale emissions modeling approaches, macroscale approaches underestimated exposure to diesel transit bus emissions because (a) total emissions of pollutants sensitive to mode were underestimated and (b) coincidence between the heterogeneous spatial distributions of emissions and impacted populations were not accounted for. As pedestrian populations proximate to the route were disproportionately impacted, these results have implications for distributional equity. Furthermore, as similar patterns in emissions rates and vehicle activity have been found across a wide range of heavy-duty and light-duty vehicles, these results may have implications for mobile sources other than diesel transit buses (15, 20, 22, 28).

Analyses at fine spatial scales are often associated with greater cost but only add value where heterogeneity exists, for example near roadways (8). Efficient and equitable mitigation of the health impacts associated with mobile source emissions requires improved characterization of the impact pathway that is sensitive to scale and heterogeneity. Microscale emissions models have greatly improved characterization of mobile source emissions; however, uncertainties in the dispersion process and the time-activity patterns of impacted populations remain and warrant further study.

Acknowledgments

This research was supported by a Scholarship from the Natural Sciences and Engineering Research Council of Canada, a Doctoral Fellowship from the University of British Columbia and grants from the Climate Decision Making Center at Carnegie Mellon University (U.S. National Science Foundation grant SES-0345798), Auto21 and Translink. We thank Dave Gourley, Dave Grabowski, Dave Leister, Alix Drapack, Milind Kandlikar, Andy Grieshop, Steve Rogak, Chris Frey, and Shahab Pichaghian.

Supporting Information Available

Detailed discussion of methods, visualizations of activity data and east-bound emissions, histograms of total emissions and total interval emissions, derivation of the spatial coincidence factor. This material is available free of charge via the Internet at <http://pubs.acs.org>.

Literature Cited

- Dockery, D. W.; Pope, C. A.; Xu, X. P.; Spengler, J. D.; Ware, J. H.; Fay, M. E.; Ferris, B. G.; Speizer, F. E. An association between air-pollution and mortality in 6 united-states cities. *N. Engl. J. Med.* **1993**, *329* (24), 1753–1759.
- Traffic-Related Air Pollution: A Critical Review of the Literature on Emissions, Exposure, and Health Effects*; Health Effects Institute/Boston. Massachusetts, 2009.
- Pope, C. A.; Dockery, D. W. Health effects of fine particulate air pollution: Lines that connect. *J. Air Waste Manage. Assoc.* **2006**, *56* (10), 709–742.
- Marshall, J. D.; Nazaroff, W. W. Intake Fraction. In *Exposure Analysis*, Ott, W. R., Steinemann, A. C., Wallace, L. A., Eds.; CRC Press: Boca Raton, FL, 2006; pp 237–251.
- Nazaroff, W. W. New Directions: It's time to put the human receptor into air pollution control policy. *Atmos. Environ.* **2008**, *42* (26), 6565–6566.
- Levy, J. I.; Greco, S. L.; Melly, S. J.; Mukhi, N. Evaluating efficiency-equality tradeoffs for mobile source control strategies in an urban area. *Risk Anal.* **2009**, *29* (1), 34–47.
- Jerrett, M.; Burnett, R. T.; Ma, R. J.; Pope, C. A.; Krewski, D.; Newbold, K. B.; Thurston, G.; Shi, Y. L.; Finkelstein, N.; Calle, E. E.; Thun, M. J. Spatial analysis of air pollution and mortality in Los Angeles. *Epidemiology* **2005**, *16* (6), 727–736.
- Greco, S. L.; Wilson, A. M.; Hanna, S. R.; Levy, J. I. Factors influencing mobile source particulate matter emissions-to-exposure relationships in the Boston urban area. *Environ. Sci. Technol.* **2007**, *41* (22), 7675–7682.
- National Research Council. *Modeling Mobile-Source Emissions*; National Academy Press: Washington, D.C., 2000.
- Kaur, S.; Nieuwenhuijsen, M. J.; Colville, R. N. Fine particulate matter and carbon monoxide exposure concentrations in urban street transport microenvironments. *Atmos. Environ.* **2007**, *41* (23), 4781–4810.
- Brugge, D.; Durant, J. L.; Rioux, C. Near-highway pollutants in motor vehicle exhaust: A review of epidemiologic evidence of cardiac and pulmonary health risks. *Environ. Health* **2007**, *6* (23).
- Barth, M.; An, F.; Norbeck, J.; Ross, M. Modal emissions modeling: A physical approach. *Transp. Res. Rec.* **1996**, *1520*, 81–88.
- Tainio, M.; Tuomisto, J. T.; Hanninen, O.; Aarnio, P.; Koistinen, K. J.; Jantunen, M. J.; Pekkanen, J. Health effects caused by primary fine particulate matter (PM_{2.5}) emitted from buses in the Helsinki metropolitan area, Finland. *Risk Anal.* **2005**, *25* (1), 151–160.
- Cohen, J. T.; Hammitt, J. K.; Levy, J. I. Fuels for urban transit buses: A cost-effectiveness analysis. *Environ. Sci. Technol.* **2003**, *37* (8), 1477–1484.
- Jackson, E.; Qu, Y.; Holmén, B.; Aultman-Hall, L. Driver and road type effects on light-duty gas and particulate emissions. *Transp. Res. Rec.* **2006**, *1987*, 118–127.
- Hallmark, S. L.; Guensler, R.; Fomunung, I. Characterizing on-road variables that affect passenger vehicle modal operation. *Transp. Res., Part D* **2002**, *7* (2), 81–98.
- Clark, N. N.; Kern, J. M.; Atkinson, C. M.; Nine, R. D. Factors affecting heavy-duty diesel vehicle emissions. *J. Air Waste Manage. Assoc.* **2002**, *52* (1), 84–94.
- Koupal, J.; Michaels, H.; Cumberworth, M.; Bailey, C.; Brzezinski, D. EPA's Plan for MOVES: A Comprehensive Mobile Source Emissions Model, *International Emission Inventory Conference*, Atlanta, GA, 2002.
- Zhai, H. B.; Frey, H. C.; Roupail, N. M. A vehicle-specific power approach to speed- and facility-specific emissions estimates for diesel transit buses. *Environ. Sci. Technol.* **2008**, *42* (21), 7985–7991.
- North, R. J.; Noland, R. B.; Ochieng, W. Y.; Polak, J. W. Modelling of particulate matter mass emissions from a light-duty diesel vehicle. *Transp. Res., Part D* **2006**, *11* (5), 344–357.
- Clark, N. N.; Gajendran, P.; Kern, J. M. A predictive tool for emissions from heavy-duty diesel vehicles. *Environ. Sci. Technol.* **2003**, *37* (1), 7–15.
- Ishaque, M. M.; Noland, R. B. Simulated pedestrian travel and exposure to vehicle emissions. *Transp. Res., Part D* **2008**, *13* (1), 27–46.
- Li, J. Q.; Zhang, W. B.; Zhang, L. A web-based support system for estimating and visualizing the emissions of diesel transit buses. *Transp. Res., Part D* **2009**, *14* (8), 533–540.
- Canadian Digital Elevation Data, Level 1 (CDED1)*, No. 092G06; GeoBase, Natural Resources Canada, Centre for Topographic Information: Sherbrooke, Quebec, 2003.
- Statistics Canada 2006 Census of Canada. <http://www12.statcan.ca/census-recensement/2006/rt-td/index-eng.cfm> (accessed April 15, 2007).
- Yanowitz, J.; McCormick, R. L.; Graboski, M. S. In-use emissions from heavy-duty diesel vehicles. *Environ. Sci. Technol.* **2000**, *34* (5), 729–740.
- Clark, N. N.; Jarrett, R. P.; Atkinson, C. M. Field measurements of particulate matter emissions, carbon monoxide, and exhaust opacity from heavy-duty diesel vehicles. *J. Air Waste Manage. Assoc.* **1999**, *49* (9), 76–84.
- Unal, A.; Frey, H. C.; Roupail, N. M. Quantification of highway vehicle emissions hot spots based upon on-board measurements. *J. Air Waste Manage. Assoc.* **2004**, *54* (2), 130–140.
- Stevens, G.; Wilson, A.; Hammitt, J. K. A benefit-cost analysis of retrofitting diesel vehicles with particulate filters in the Mexico City metropolitan area. *Risk Anal.* **2005**, *25* (4), 883–899.
- Zhou, Y.; Levy, J. I. Factors influencing the spatial extent of mobile source air pollution impacts: a meta-analysis. *BMC Public Health* **2007**, *7* (89).

ES101391R